

Krzysztof ROGOWSKI^{1*}
Jakub PAWLICKI¹

NUMERICAL ANALYSIS OF THE STEAM FLOW PAST THE TURBINE BLADE STAGE

The steam flow past a last stage (the eleventh stage) of the high pressure part of the TK120 steam turbine was investigated using computational fluid dynamics (CFD). The simulations are performed using the unsteady compressible Navier-Stokes equations. Viscous steam flow has been analyzed using the Spalart-Allmaras turbulence model. The paper presents distributions of instantaneous flow parameters around turbine blades as well as instantaneous aerodynamic blade loads. Flow parameters such as: velocity and static pressure are presented as contour maps whereas aerodynamic loads, axial and circumferential, are given as functions of time. Theoretical power of the examined turbine stage is 4.11 MW. Based on the numerical investigations the power of the analyzed stage is evaluated to be 3.5 MW. All presented in this paper results have been performed using the ANSYS Fluent solver.

1. INTRODUCTION

Steam turbines are in fact turbo-machines and they are used in almost all industrial systems [1]. In contrast with an internal combustion engine, fluid (e.g. steam) is heated in a separated device such as steam boilers or nuclear reactors [2]. Steam turbines can be divided into impulse turbines and reaction turbines. In the impulse-type turbines steam expands in expansion devices (e.g. stator blades) whereas in the reaction-type turbines steam expands also between the rotor blades. The first impulse-type turbine was created by Laval in 1883. Principle of operation of the steam turbine depends on conversion of thermal energy of steam into kinetic energy of the steam and then into mechanical work of a rotating output shaft of the turbine. The steam flow through the rotor blades is associated with a decrease in enthalpy of steam. Rapid development of steam turbines, also in Poland, took place after the Second World War. Steam turbines can operate with steam boilers or nuclear reactors in power units. They are produced ranging from small size units (< 0.75 kW) to large turbines (1.5 GW). The smallest steam turbines are used as mechanical drivers for pumps, compressors etc. whereas large turbines are usually used to generate electricity [3],

¹ Warsaw University of Technology, Faculty of Power and Aeronautical Engineering, Warsaw, Poland

* E-mail: krogowski@meil.pw.edu.pl

[4]. Steam turbines are still innovated and modified and they are responsible for the energy system of many countries [5].

Computational fluid dynamics codes solve Reynolds Averaged Navier-Stokes (RANS) equations in defined computational domains. As a result, these methods can be used to analyse extremely complex flows. However, studies using CFD methods are rather rare in the steam turbine applications due to the high cost of computing. The flow past a turbine blade passage is complex and three-dimensional. However, CFD analysis can help understanding the flow behaviour in different parts of steam turbines. This is important in order to more accurately assess the turbine performance and distribution of flow parameters such as e.g.: pressure, temperature, velocity etc. Computational fluid dynamics (CFD) was used by Sakai et al. to compute partial admission stages in steam turbines. Authors performed quasi-3-dimensional (Q3D) simulations of the mean radius in order to reduce computing costs [6]. Basavaraj and Shashishekar used the Spalart-Allmaras turbulence model to reprofiling and optimization of a 50% reaction turbine blade profile [7]. Numerical experiments of these authors were also performed using Q3D CFD. Swirydczuk investigated the interaction between the stator wakes and the rotor turbine blades in a turbine stage.

This stochastic phenomenon was taken into account in computations of RANS equations [8],[9]. Kim et al. investigated a single rotor of a 500 MW fossil-fuel power plant using CFD. Large Eddy Simulations (LES) was employed by these authors to predict the unsteady loading on the blade surface under partial admission [10]. Segawa et al. studied the impact of changes in blade rotor geometry on aerodynamic blade loads of a steam turbine [11]. Computational fluid dynamic software was used by Campos-Amezcuca et al. who study of erosion due to solid particles in steam turbine blades [12].

The purpose of the paper is the analysis of instantaneous pressure distributions on the turbine blades as well as the averaged pressure and velocity distributions on the blades employing the Spalart-Allmaras turbulence model.

2. STEAM TURBINE PARAMETERS

The TK120 is three-casing impulse-type condensing steam turbine with steam reheat, and six-stage regeneration system powered by bleed steam. The rated power of the turbine is 120 MW and the rotational speed is 3000 rpm. Service time of such steam turbines is very long (e.g. the investigated turbine has operated since 1969 for 35 years). Since production of new machines is expensive and energy-consuming [113] a number of structural and flow analyses were made for the existing turbine TK120. The scope and purpose of work was consulted in cooperation with ZRE “Katowice” company. Numerical analyses of the 11th stage (the last stage) of the high pressure part of the TK120 steam turbine have been performed based on turbine specifications and the technical report [14].

Presented in the paper simulations are performed for the steam parameters given in Table 1. Silhouette of the rotor disc of the 11th turbine stage is shown in Fig. 1, whereas the geometry of the turbine blade is presented in Fig. 2.

Table 1. Steam parameters used during simulation at the 11th stage of the HP part of the TK120 turbine

Parameter	Value
Steam pressure at the stage inlet	3.3 MPa
Steam temperature at the stage inlet	351°C
Steam pressure at the stage outlet	2.9 MPa
Steam temperature at the stage outlet	333°C

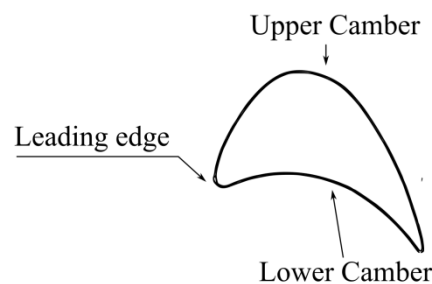
Fig. 1. Rotor disc of the 11th turbine stage

Fig. 2. Profile of the turbine blade

3. CFD MODEL

A geometrical model of the fixed and moving blades of the turbine has been developed based on the technical drawings. In the high pressure part of the steam turbine the fixed and rotating blades are very short therefore during simulations only the two-dimensional model of the blades have been considered. In order to create the two-dimensional model the plane of the blades has been formed by expanding the arc coordinate located on the pitch diameter of the turbine rotor disc. The distance between blades was determined based on the number of blades and the pitch diameter of the turbine rotor disc. Since the two-dimensional flow was established, the length of the analysed area should be infinitely. Geometrical model of infinite length, however, is not possible to create therefore on the boundaries of computational domain, the periodicity condition has been assumed. In addition, the remaining boundaries of computational domain such as the velocity inlet and pressure outlet are presented in Fig. 3.

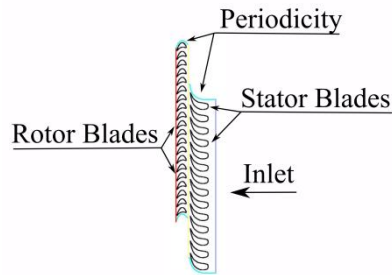


Fig. 3. CFD model of the turbine stage

The investigated area around the turbine blades is divided into finite elements. During simulations a hybrid mesh consisting of structural quadrilateral elements near the turbine edges and unstructured triangle elements elsewhere is used. The structural mesh is created to simulate boundary layer effects. Elements of this mesh have a very low height near the edges of the blades and grow as they move away from the edges. Fig. 4 presents the grid used during CFD simulations. This mesh consists of 341 014 elements and 300 456 nodes. In order to correctly simulate the viscosity-affected region of the boundary layer a near-wall region should be properly modelled. According to the ANSYS, Inc.15.0 documentation in order to avoid computational errors a non-dimensional wall distance for wall-bounded flow y^+ should be ≤ 1 . Table 2 gives y^+ parameters for turbine and stator blades.

Table 2. Non-dimensional wall distance

	y^+
Rotor blades	0.45-1.02
Stator blades	0.80-1.00

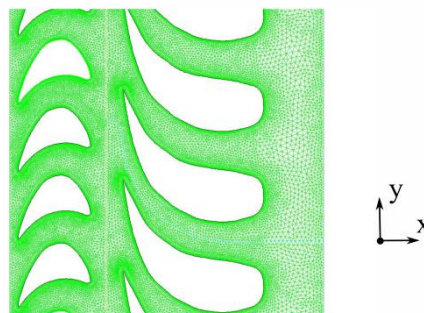


Fig. 4. Mesh

All simulations presented in the paper have been performed using a mesh presented in Fig. 4. The total number of mesh points on the blades of the rotor and stator are 100 and 150 respectively. In order to examine the effect of mesh resolution on the numerical solution three meshes with different cell densities have been implemented. These three grids differ in the number of mesh points at the edges of the blades. Parameters of these grids are given in Table 3.

Table 3. Three meshes with different number of grid points at the turbine blade N_t and at the stator blade N_s

	N_t	N_s
Mesh A	70	120
Mesh B	100	150
Mesh C	130	180

Table 4 shows the results of averaged values of circumferential force \bar{F}_y and axial force \bar{F}_x for three meshes given in the Table 3. The differences between aerodynamic load components computed for the coarse and finer meshes are very low.

Table 4. Aerodynamic force components for three mesh

	\bar{F}_y	\bar{F}_x
Mesh A	152.8146	53.8888
Mesh B	154.6230	54.7515
Mesh C	154.7604	54.8001

All presented in the paper numerical results have been performed using the ANSYS Fluent solver. Unsteady compressible Navier-Stokes equations are used to simulate steam flow past the turbine blades. The solved system of equations consists also of the energy equation. Steam is assumed to be viscous fluid and therefore the turbulence model is chosen. In order to reduce computing time, the one-equation Spalart-Allmaras turbulence model is used. The movement of the turbine rotor is modelled through the application of sliding mesh technique. This technique handles the physical movement of the turbine rotor through the movement of the assigned mesh area that represents the rotor. The mesh of the moving part of the turbine stage moves relative to the stationary stator mesh. Translational velocity of the rotor mesh corresponds to the tangential velocity of the rotor at the pitch diameter of the disc.

The Spalart-Allmaras turbulence model solves a transport equation for the kinematic eddy viscosity. The simple model was developed for aerospace applications where flow is attached to the analysed body. This model is also popular in turbomachinery applications. The Spalart-Allmaras model, available in the ANSYS Fluent solver is not adapted (calibrated) for general industrial flows, therefore it can generate significant computational errors for some free shear flows.

The numerical results of aerodynamic loads and flow parameters presented in the paper are preliminary. For more accurate simulations more advanced turbulence models are recommended. Such models are, for example the $k-\varepsilon$ and the $k-\omega$ turbulence models. Those models in combination with enabled wall functions provide satisfactory results.

4. AERODYNAMIC LOADS

Aerodynamic blade loads, circumferential force F_y and axial force F_x , are computed using CFD based on pressure distributions around blades. The aerodynamic blade loads

vary periodically in time. Fluctuations of aerodynamic load components are caused by rotor blades that move one near the leading edge of a fixed stator vane and one in the area between the stator vanes. The paper presents both the aerodynamic blade loads fluctuations and averaged values of these blade loads. Averaging time corresponds to the distance that the turbine blade passes between the three neighbouring stator vanes.

The torque of a single rotor blade T_i depends on the pitch diameter of the turbine disc D_P and the averaged value of the circumferential force \bar{F}_y :

$$T_i = \frac{1}{2} D_P \cdot \bar{F}_y \quad (1)$$

The torque of the turbine disc T is a sum of torques of all blades (n blades) of the rotor disc:

$$T = \sum_{i=1}^n T_i \quad (2)$$

The power generated by a single turbine stage depends on the torque T and the angular velocity of the rotor ω :

$$P = T \cdot \omega \quad (3)$$

5. RESULTS AND DISCUSSION

Fig. 5 presents aerodynamic blade load components, circumferential force F_y and axial force F_x as a function of time t . Time interval $3.65e-4$ seconds corresponds to the distance travelled by the rotor disk blade between the three neighboring stator vanes. As can be seen from this figure, the circumferential force acting on a single blade varies from 144 N to 165 N. The difference between the maximum and the minimum value of this force is only 21 N. The axial force F_x varies in the range of 52.1 N and 57.5 N. The averaged value of this force component is equal to 54.75 N and it is lower by 64.6% than the average value of the circumferential force.

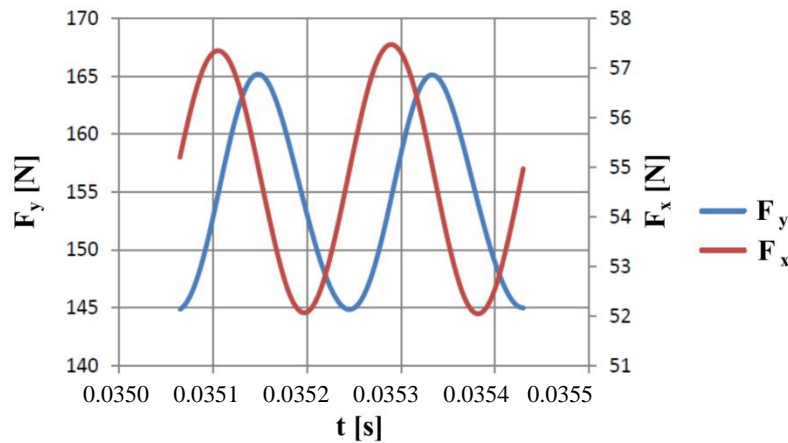


Fig. 5. Aerodynamic blade loads, circumferential F_y and axial F_x

Static pressure distributions around the rotor disc blade at four different instants are presented in Fig. 6. Every moment of time corresponds to the displacement of the rotor disc blade equal to 1/4 of the distance between two neighboring stator vanes. The impact point corresponds to the static pressure is constant for all presented here instants. Analysing presented in the paper instantaneous static pressure distributions it has been found that the differences between pressure characteristics are very small. The small differences between these characteristics are observed at both edges of the blade in the middle of the blade.

Presented in Fig. 6 static pressure is given as a function of position that is the position of the blade profile points in the global coordinate system. The beginning of the global coordinate system is located behind the profile of the turbine rotor blades. Point on the graph furthest away from the beginning of the coordinate system corresponds to the leading edge of the turbine blade.

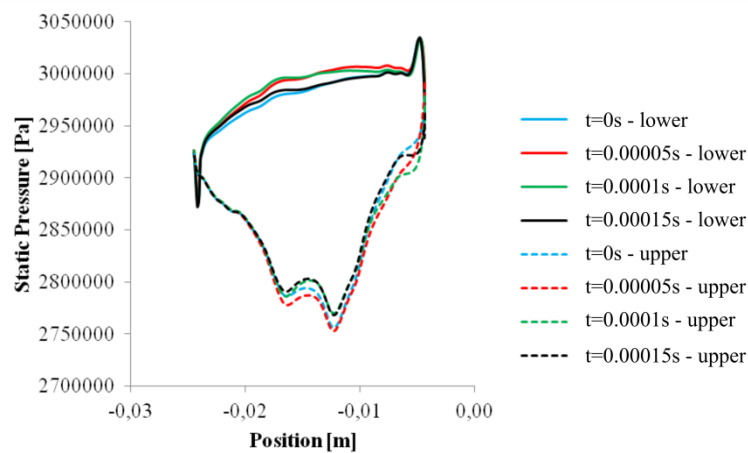


Fig. 6. Static pressure for upper and lower cambers at four instants

Fig. 7 presents the contour maps of static pressure and velocity magnitude. It is shown in the previous paragraph that changes in the instantaneous flow parameters are small therefore results presented in Fig. 7 are given only for one instant. Analysing these figures it can be observed expansion of steam on the stator vanes.

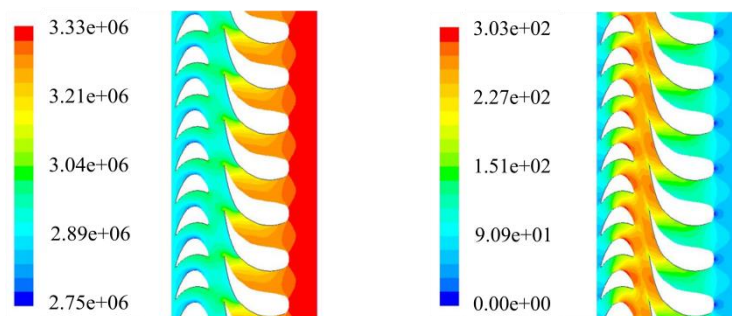


Fig. 7. Contour maps of static pressure (on the left) and velocity magnitude (on the right). Pressure is given in Pascal whereas velocity in meter per second

In order to compute the turbine stage power the torque of the disc is computed by using the integrated value of the circumferential force F_y and half of the pitch diameter D_p . Based on the numerical computations, the averaged circumferential force \bar{F}_y for one blade is 135.63 N. The power of the 11th stage of the high power part of the steam turbine is 3.5 MW. Theoretical power of this stage is 4.11 MW and therefore the efficiency of the turbine stage is 85%.

Analysis of unsteady flow past a steam turbine is computationally expensive. Moreover the use of the density-base solver increases the computational cost. The calculations presented in this article were made by HP Dual Xeon CPU's 2.8 GHz computer supplied with 4.0 Gb of RAM.

6. CONCLUSION

In this paper the results of aerodynamic blade loads, the turbine stage torque and the internal efficiency of this turbine stage are presented. All presented in this paper results are computed using the Spalart-Allmaras turbulence model. Obtained numerical results are not compared with other, more complex, turbulence models such as the k- ϵ or the k- ω . Firstly, this paper presents only preliminary CFD computations of the steam turbine. Secondly, more complex turbulence models increase the cost of computing. The comparison of all available in the ANSYS Fluent turbulence models requires the use of multiple processors, even for the case of two-dimensional flow. Moreover, experimental data of aerodynamic loads, turbulence, velocity components etc. for investigated steam turbine is not available.

The averaged value of the circumferential force is equal to 54.75 N and it is lower by 64.6% than the average value of the circumferential force. Based on the numerical computations, the efficiency of the investigated turbine stage is estimated at 85%. Based on numerical results presented in the paper it was found that the simple one-equation Spalart-Allmaras turbulence model can be used in heat flow problems of steam turbines.

The movement of the 2D rotor is modelled by using the sliding mesh technique. It is recommended to perform a 3D model of the rotor. The use of such model as well as the sliding mesh approach provides satisfying results.

ACKNOWLEDGMENTS

This work was financed by Polish NCBR, project POIG, project 1.3.1-14-074 / 12, task 4.

REFERENCES

- [1] CHRZANOWSKI W., 1929, *Modern steam turbines*, Warszawa, (in Polish).
- [2] ŚWIRYDCZUK J., 2013, *Wake-blade interaction in steam turbine stages*, Polish Maritime Research, 20/2(78), 30-40.

-
- [3] NIKIEL T., 1989, *Steam turbines*, Wydawnictwa Naukowo-Techniczne, Warszawa, (in Polish).
- [4] BASAVARAJ H.N., SHASHISHEKAR K.S., 2013, *Reprofiling and optimization of a 50% reaction turbine blade profile for HP steam path*, International Journal of Advanced Scientific and Technical Research, 3/4, 137-153.
- [5] ŚWIRYDCZUK, J., 2006, *CFD modelling of turbine stage stator/rotor interaction*, TASK Quarterly, 10/2, 113-124.
- [6] SEGAWA K., SHIKANO Y., TSUBOUCHI K., SHIBASHITA N., 2002, *Development of highly loaded rotor blade for steam turbines*, Japan Society Mechanical Engineering (JSME) International Journal Series B, 45/4, 881-890.
- [7] CHMIELNIAK T.J., 1993, *Fluid-flow machines*, Wydawnictwo Politechniki Śląskiej, Gliwice, (in Polish).
- [8] CAMPOS-AMEZCUA A., MAZUR Z., GALLEGOS-MUNOZ A., ROMERO-COLMENERO A., RIESCO-AVILA J.M., MEDINA-FLORES J.M., 2008, *Numerical study of erosion due to solid particles in steam turbine blades*, Numerical Heat Transfer, Part A, 53, 667-684.
- [9] RUSEK P., WANTUCH E., ZAGÓRSKI K., 2013, *The problem of energy-consuming processes in the planning of modern manufacturing technologies*, Journal of Machine Engineering, 13/4, 68-76.
- [10] SAKI N., HARADA T., IMAI Y., 2006, *Numerical study of partial admission stages in steam turbine (Efficiency improvement by optimizing admission arc position)*, JSME International Journal Series B Fluids and Thermal Engineering, 49/2, 212-217.
- [11] DEMBIŃSKI K., 2013, *Computations of distribution of steam parameters in the high-pressure part of the TK-120 turbine*, Technical report, Katowice.
- [12] PERYCZ S., 1992, *Steam and gas turbines*, Wydawnictwo Polskiej Akademii Nauk, (in Polish).
- [13] KIM H., LEE H., KIM D., BOSE S.T., PHILIPS D.A., 2014, *Prediction of unsteady loading on a steam turbine blade*, Center for Turbulence Research, Proceedings of the Summer Program, 479-487.
- [14] PROŚ D., ZABORSKI S., 2010, *Analysis of the wire electrical discharge machinability of roots of steam turbine blades*, Journal of Machine Engineering, 10/1, 70-77.